International Journal of Latest Research in Engineering and Technology (IJLRET)
ISSN: 2454-5031
www.ijlret.com || Volume 02 - Issue 09 || September 2016 || PP. 67-74

Galvanostatic co-electrodeposition of Cu/Pd on Ti as catalyst for nitrates reduction in water

Bren Mark Felisilda[1], Kyoung Young Eum[2], Jin Woo Kim[2]
Jang Myoun Ko[1], Changwoo Park[1,¶],

[1]*Department of Chemical and Biological Engineering, Hanbat National University, San 16-1 Deokmyeong-dong, Yuseong-gu, Daejeon 305-719, South Korea*
[2]*HanKook Tech (#507, Migun Techno World 1) 199, Techno 2-ro, Yuseong-gu, Daejeon, 34025, South Korea*

[¶]Corresponding Author: Changwoo Park

Abstract: The galvanostatic co-electrodeposition of copper and palladium on titanium is studied using cyclic voltammetry and linear sweep voltammetry. The optimized current density and time for co-electrodeposition is found to be 7 mA/cm^2 for 7200 seconds. The prepared electrocatalyst showed promising efficiency of reducing nitrates in the range of 95-98 % from an original concentration of 100 ppm. SEM images reveal the surface deposits to be amorphous with cauliflower-like structures and the EDX analysis show deposition of the Cu/Pd on the Ti substrate. The reduction efficiency of the catalyst was enhanced by 2-3% with an addition of Na_2SO_4 as a supporting electrolyte. Soaking the prepared electrodes in tap water for 14 weeks caused detrimental effects on its nitrate reduction efficiency.

Keywords: galvanostatic electrodeposition; Cu/Pd bimetallic; electrochemical reduction; nitrates

1. Introduction

The problem of contaminated water resources has been a recurrent dilemma for mankind. Nitrate contamination, mainly caused by fertilizer misuse and industrial waste, is receiving much attention due to its health hazards [1]. Therefore, it is necessary to reach the allowed concentration for proper disposal into the environment. The well-known nitrate removal method for practical application involves biological processes but parameters in this technology require constant maintenance [2]. Other known technologies like ion exchange and reverse osmosis require further additional treatment while conventional coagulation techniques still make use of additional reagents that significantly increase the salinity of the water [3]. To address these problems, electrochemical techniques have become important alternatives for nitrates reduction because of less chemicals used, low cost and good efficiency [4]. One example is electrocoagulation, which was found to be efficient in removing nitrates using aluminum and iron electrodes [5-7]. In addition, many literatures on electrolytic reduction of nitrates are available. These include the use of monometallic catalysts like Ni, Ti, Pb, Zn, Rh but bimetallic catalysts are found to be more effective in reducing nitrates in water [8-14]. Bimetallic catalysts, generally composed of a noble metal (eg. Au, Pt, and Pd) combined with a second metal that serves as a promoter (eg. Sn, Cu, and Ni), were widely investigated. Over the years, various bimetals (alloy) such as Cu/Zn, Pd/Cu, Ti/IrO_2, BDD, Pb, Ni, and Pt [8-14] have been probed as catalytic electrodes for nitrate reduction.

Presently, the more efficient catalysts are Pd-Cu on various substrates or supports. The methods of preparing such catalysts include electrodeposition, electroless plating and other conventional techniques [10, 14-16]. Milhano and Pletcher, [10] as well as Allemandet *et al* [14] were able to co-electrodeposit Pd-Cu alloys over a wide range of composition from sulfate-based and nitrate-based baths respectively. These and other studies involving co-electrodeposited Cu/Pd alloys made use of a three-electrode system, meaning a constant voltage was applied to deposit the two metals on the surface of the substrate.

The main interest of this study is to galvanostatically co-electrodeposit Cu and Pd on titanium substrate and its catalytic activity on nitrate reduction is investigated. As of the moment, not many studies are making use of co-electrodeposited Pd/Cu alloys as electrodes for nitrate reduction.

2. Experimental

2.1 Materials

All aqueous solutions prepared in this study were made with distilled water from AquaMax Ultra (Younglin Instruments Inc.; resistivity 18.2 MΩ*cm). The deposition solution bath was made consisting of 8

mM $CuCl_2$ + 5 mM $PdCl_2$ in 0.5 M HNO_3. Synthetic nitrate solutions with initial concentration of 100 mg/L were prepared using KNO_3 (Oriental Chemical Industries, Korea) in distilled water. Most chemicals were purchased from Sigma Aldrich Corporation or otherwise mentioned.

2.2 Electrocatalyst Preparation

Titanium foil with an active area of 1x1 cm^2 was used as the substrate for electrodeposition. Prior to electrodeposition, the titanium foils were first polished with silicon carbide, waterproof abrasive paper then cleaned in hot (80° C) 1 M $HCl_{(aq)}$ solution and then wash with distilled water. Again the electrodes were agitated in acetone using an ultrasonic bath for 15 min and finally rinse with distilled water. Deposition baths were stirred at 500 rpm before deposition.

2.3 Electrochemical Measurements

All electrochemical measurements were performed in a three-electrode, one compartment cell at room temperature (25±1 °C). A platinum electrode is used as a counter electrode and saturated Ag/AgCl as a reference electrode, thus all potentials reported is referenced to its potential.

2.4 Electrocatalyst Characterization

The surface morphology of the metals deposited and their concentration were examined using a field emission scanning electron microscope (FE-SEM, model HITACHI S-4800) at an accelerating voltage of 20 kV and energy dispersive X-ray spectroscope (EDXS, model EX-250 Horiba) attached to the FE-SEM.

2.5 Electroreduction of Nitrates in Water

Approximately 5 mL of the prepared nitrate solution is then poured into the electrochemical cell after which a constant current density is applied (12 mA/cm^2) for a total time of 3 hours. At different time intervals, 1 mL sample was drawn from the electrochemical cell for analysis. Nitrate concentration was then analyzed using a UV-VIS (MECASYS UV-Vis Spectrophotometer) colorimetric method at 410 nm utilizing the rapid determination of nitrate-N by complexation [17].

3. Results and Discussion

3.1 Determination of current density and optimization

The current density was optimized to obtain the current density that will yield better catalyst for excellent nitrate reduction efficiency. Table 1 depicts the current densities and their corresponding deposition time for the deposition of Cu/Pd on Ti foil. Electrode C with a current density of 7 mA/cm^2 and a deposition time of 7200 s demonstrated the highest removal efficiency of 98.5% compared to the other electrodes. Furthermore, increasing the current density above 7 mA/cm^2 resulted in a decrease in reduction efficiency. This implies that the 7 mA/cm^2 current density was sufficiently enough to obtain a pure Cu/Pd bimetallic deposition with a thickness of 1-5 μm.

To better understand the electrocatalytic activity of the galvanostatically prepared electrodes, and whether deposition occurred on the cathodic or anodic electrode, the surfaces of the prepared electrodes were studied using scanning electron microscopy which is coupled with energy dispersive x-ray spectroscopy to identify species on the surface. Figure 1a-d exhibits the SEM micrographs obtained from the normal positioning and reversed positioning. Normal positioning refers to having the working electrode as the cathode while the counter electrode as the anode. The opposite is true for the reversed position. Co-electrodeposition was done using an aqueous solution of 8 mM Cu + 5 mM Pd in 0.5 M HNO_3 as depositing bath at a current density of 20 mA/cm^2 for 500s as preliminary conditions, based on a reference study [16]. The SEM micrograph of the Cu/Pd bimetallic alloy reveals dome-like, rough and porous structures on the anode in normal position while it is shown on the cathode in the reversed position. The EDX profiles of the previously mentioned SEM micrographs are displayed in Figure 2, and it further validates that the major species on the electrode surface after deposition were Cu/Pd particles. The elemental compositions are as follows: In the normal position, (a) working electrode surface has $Ti_{0.73}O_{4.08}$, (b) counter electrode has $Ti_{0.26}Cu_{0.45}Pd_{0.12}$ while on the reversed position, (c) working electrode surface has $Ti_{0.76}Cu_{0.38}Pd_{0.21}$ and (d) counter electrode has $Ti_{0.73}O_{4.03}$. This implies that the co-electrodeposition of Cu/Pd on the Ti foil surface is possible using constant current method.

3.2 Electrochemical measurements and electrodeposition

Figure 3 reports the voltammograms of the prepared electrocatalyst in just the supporting electrolyte (a) and in the presence of 100 ppm nitrate solution (b). As observed in the figure mentioned, reduction current is observed in both (a) blank and (b) KNO_3 solution when the potential was lower than -0.4 V versus Ag/AgCl. This could be a result of the electrolysis of water into hydrogen, which is the main process observed in this part.

However, a visible peak around -0.65V is noticed in the presence of nitrate ions in solution (b). This can be linked to nitrate reduction as discussed by Wang and Qu [18] in their study on palladium-modified copper electrodes.

Linear sweep voltammetry measurements were also carried out to investigate the possible effect of the scan rate on the shape of the voltammograms obtained, which can later help us describe the Cu/Pd alloys formed qualitatively. Voltammograms of such measurements are shown in Figure 4. No peak is visible for (a) the voltammogram produced by the Ti foil in the 0.5 M HNO_3. The positions of the two curves are the same with the different scan rates. In the presence of 8 mM Cu in 0.5M HNO_3, voltammogram displayed in (b), shows a visible peak around 0.4 - 0.2 V. This first peak signifies the reduction of Cu^{2+} to metallic copper deposited on the Ti surface [15]. The intense peak that begins at a more positive potential can be associated with the underpotential deposition (UPD) of Cu [13]. Cu deposition continues to 0.0 V and a significant hysteresis is seen which is consistent with the Cu deposition reaction involving nucleation and possible growth of Cu layer.

The more obvious effect of scan rate is shown in (c) the voltammogram from the Ti foil in the presence of 5 mM Pd in 0.5 M HNO_3. At a higher scan rate, the peaks are shifted to a more positive potential. This can be explained by the fact that as the scan rate increases, the total current is also increased. This can be understood by considering the size of the diffusion layer and the length of time to record the complete scan. Clearly, if scan rate is low, more time is required. Therefore, the size of the diffusion layer above the electrode surface will grow much further from the electrode as compared to a faster scan. As a consequence, the flux to the electrode surface is relatively smaller at slower scan rates. Moreover, the shift of the peak can also be attributed to the idea that the system is quasi-reversible, where the rate constant can alter the shape of the voltammogram [19]. At 20 mV/s, peaks were visible at -0.1 V and -0.3 V while at 50 mV/s, these become more positive at -0.05 V and -0.2 V. The peak around -0.05 V can be related to the underpotential deposition (UPD) of hydrogen on the Pd surface. Also, as suggested by prior studies by Birry *et al* [20] and Duncan *et al* [21], the second peak at about -0.3 to -0.2 V as well as the reduction wave past these potentials are linked to H absorption and the hydrogen evolution reaction (HER) at the Pd surface.

3.3 Characterization of Deposits

Figure 5a reports the SEM images of films obtained by co-electrodeposition using galvanostatic mode. The chemical composition was simultaneously determined by EDX. All the Cu/Pd films presented a porous and cauliflower-like structure. The morphologies of pure Pd (dendritic deposits) and pure Cu (large crystals) films are very different from each other and from that of the Cu/Pd alloy films. Also, as seen in the images most electrodeposited coatings completely cover the Ti foil substrates. From other studies, it has been concluded that the surface morphologies of the deposits depend on the composition of the deposition bath and therefore the film stoichiometry [1]. However, this study did not look at the specific individual ratios for the morphological studies but rather the ratios presented here are based on the EDX results of the more viable spot on the surface of the electrode. As mentioned above, the Cu/Pd films produced cauliflower-like structures that are dome in shape and are amorphous. Figure 5b shows the EDX profile of the electrode prepared by galvanostatic co-electrodeposition with a surface combination of $Ti_{0.76}Cu_{0.38}Pd_{0.21}$. Both EDX and SEM analyses demonstrate that Cu/Pd alloys can also be deposited galvanostatically on Ti substrates over various composition ranges. Moreover, alloying of Cu and Pd reduces the crystallite size and thus induces the formation of nanoscale structures, which can be of good value for electrocatalysis and surface applications [12].

3.4 Effect of electrolyte and kind of water used for test solution

The effect of supporting electrolyte was tested using Na_2SO_4 and NaCl. Generally, electrolytes are added to increase the conductivity of the solution. NaCl which contains Cl^- ions is regarded by other studies to be efficient in reducing nitrates in water. As shown in Figure 6a, the results gave similar results as in the case of NaCl when Na_2SO_4 was used as the supporting electrolyte and amazingly, the synthesized nitrate solution without a supporting electrolyte gave reduction efficiency close to the ones with the supporting electrolyte. This excellent performance may be attributed to the electrocatalyst superior ability to selectively reduce nitrate in both electrolyte supporting and non-electrolyte supporting nitrate wastewater. Furthermore, tap water and deionized water was used to synthesize the nitrate wastewater and the catalytic electrodes efficiency toward nitrate reduction tested in these waters. Figure 6b is the summary of the average results. The electrode demonstrated better performance in the synthesized wastewater with distilled water than in tap water. This may be due to the presence of impurity ions in the tap water that seems to poison the surface of the active electrocatalysts.

3.5 Effect of Soaking

The Cu/Pd coated Ti substrate was subjected to prolong soaking and it effectiveness towards nitrate reduction was investigated after every week. Figure 7 shows the summary of the results of the tests after the 14th week with weekly catalysis to reduce nitrates at 12 mA/cm^2 for 2 hours. The efficiency was an average of 95-98% for the first week but slowly decreased over time. In addition, Figure 8 shows the EDX images of the prepared electrodes prior and after soaking in tap water for 14 weeks with weekly catalysis to reduce nitrates at 12 mA/cm^2 for 2 hrs. From the images, changes in elemental composition can be observed over time especially when soaked in tap water. The surface composition changes from (a) $Ti_{0.76}Cu_{0.38}Pd_{0.21}$ to (b) $Ti_{1.02}Cu_{0.17}Pd_{0.07}$. This shows that prolong use may also cause some of the catalyst to fall off the substrate and affect the ability of the electrocatalyst but it is worth knowing that the electrode retained about 67% of its reduction efficiency after the 14th week. Implying that with all these little drawbacks, additional process control maybe required to achieve better efficiency.

4. Conclusion

A Cu-Pd bimetallic electrocatalyst was prepared via galvanostatic co-electrodeposition from optimized composition of 8 mM $CuCl_2$ + 5 mM $PdCl_2$ in 0.5 M HNO_3 on Ti foil. A constant current of 7 mA/cm^2 was used for the deposition for 2 hours. For the electroreduction of nitrates, the optimized current density was 12 mA/cm^2 and a catalysis time of 3 hours. Surface morphological analysis revealed that the prepared electrocatalysts has an amorphous surface with dome-like structures which are also similar to those previously prepared in potentiostatic mode (data not shown). This reveals that such surfaces are indeed a promising answer for the electroreduction of nitrates in water. Results show that soaking electrodes in water for weeks decreases the reduction efficiency to an extent due to the changes in elemental composition of the electrocatalyst. However, the reasons behind these changes are still not clear. Further stability studies of the electrocatalyst surface may answer such questions. Lastly, the electrocatalyst prepared in galvanostatic mode demonstrate better removal efficiency.

References

[1]. S.K. Gupta, A.B. Gupta, R.C. Gupta, A.K. Seth, J.K. Basain and A. Gupta, *Environ. Health Perspect.*, **108**, (2000) 363.
[2]. S. Ghafari, M. Hasan and M. K. Aroua, *Bioresource Tech.* **99** (2008) 3965
[3]. M.I. Aguilar, J. Saez, M. Llorens, A. Soler, and J.F Ortuno, *Water Res.*,**36,** (2002) 2910
[4]. L. Szpyrkowicz, S. Daniele, M. Radaelli, S. Specchia, *Appl. Catal. B: Environ.* **66** (2006) 40
[5]. A.S. Koparal, U.B. J. Ogutveren, *Hazard. Mater.*, **B89,** (2002) 83.
[6]. C.H. Huang, L. Chen, C.L. Yang, *Sep. Purif. Technol.* **65**, (2009) 137
[7]. N.S. Kumar, S. Goel, *J. Hazard. Mater.*,**173** (2010) 528.
[8]. A. Devadas, S. Vasudevan, F. Epron, *J. Hazard Mater.*, **185** (2011) 1412.
[9]. O.S.G.P. Soares, J.J.M Orfao, J. Ruiz-Martinez, J. Silvestre-Alberto, A. Sepulveda-Escribano, M.F.R Pereira, *Chem. Eng'g J.,***165** 78(2010).
[10]. C. Milhano, D Pletcher, *J. Electroanal. Chem.* **614** (2008) 24.
[11]. Y. Wang, J. Qu, R. Wu, P Lei, *Water Research.*,**40** (2006) 1224.
[12]. U. Prusse,; K.D. Vorlop, *J. Mol. Catal. A: Chem.*, **173**, (2001) 313.
[13]. J.T. Matsushima, V.C. Fernandes, A.R. Couto, M.R. Baldan, N.G Ferreira, *Inter. J. Electrochem.*, **1D**, (2012).
[14]. *M Allemand, MH Martin, D Reyter, L Roué, D Guay, C Andrei, GA Botton. Electrochimica Acta,*.**56**, (2011) 7397.
[15]. D. Reyter, D. Belanger, L. Roue, *J. Phys. Chem. C*,**113** (2009) 290.
[16]. M. Li, C. Feng, Zhang, Z. Yang, S. Suguira, N. *Bio. Tech.* **101** (2010) 6553.
[17]. D.A. Cataldo, M. Maroon, L.E. Schrader, V.L. Youngs, *Commun. Soil Sci. Plan.*, **6**, 71(1975).
[18]. Y. Wang, J. Qu, *Water Environ. Res.*,**78** (2006) 724.
[19]. W.J. Plieth, in: Bard, A.J. (Ed.), Encyclopedia of Electrochemistry of the Elements, vol. 8, Marcel Dekker, New York (1978)
[20]. L. Birry, A. Lasia, Electrochem. Acta, 51 (2006) 3356.
[21]. H. Duncan, A. Lasia, Electrochem. Acta, 53 (2008) 6845.

Tables

Table 1 Electrocatalyst prepared with varying current densities and deposition time.

Table 2 Percent efficiencies of the various electrodes prepared in various current densities but constant reduction current during catalysis

Figure Captions

Figure 1 SEM images of the (a) working and (b) counter electrodes in the normal positioning and (c) working and (d) counter electrodes in the reversed positioning.

Figure 2 EDX profiles of the (a) working and (b) counter electrodes in the normal positioning and (c) working and (d) counter electrodes in the reversed positioning.

Figure 3 CV curve at 10 mV/s of the (a) Ti-Cu/Pd electrocatalyst in 0.5 g/L Na_2SO_4 only and (b) in 0.5 g/L Na_2SO_4 + 100 ppm NO_3 solution.

Figure 4 CV curves of Ti foil in (a) 0.5 M HNO_3, (b) 8 mM Cu + 0.5 M HNO_3 (c) 5 mM Pd + 0.5 M HNO_3 at varied scan rates.

Figure 5 SEM Images of the Ti-Cu/Pd on surface by constant current method of 7 mA/cm^2 for 7200 sec; (a-5.00 µm; b-1.00 µm)
Figure 6 Plot of catalyst efficiency with respect to (a) kind of water (b) added electrolytes.

Figure 7 Electrodes efficiency after being soaked in tap water for 14 weeks with weekly catalysis in reducing nitrates.

Figure 8 SEM EDX profiles of (a) Ti-Cu/Pd before and (b) Ti-Cu/Pd after soaking for 14 weeks with weekly 2-hour catalysis.

Table 1

Electrode	Current Density/ $mAcm^{-2}$	Deposition time/ seconds	% Efficiency
A	3	7200	35.7
B	6	7200	78.1
C	7	7200	95.8
D	7.5	7200	83.2
E	8	7200	75.3

Table 2

Electrode Prep, Current/time	Catalysis, Current/time	Conc./ppm after catalysis	% Efficiency
7 mA/7200 s	12 mA/10800 s	4.238	95.8
14 mA/3600 s	12 mA/10800 s	10.376	89.6
7.5 mA/7200 s	12 mA/10800 s	16.812	83.2
15 mA/3600 s	12 mA/10800 s	8.693	91.3

Figure 1

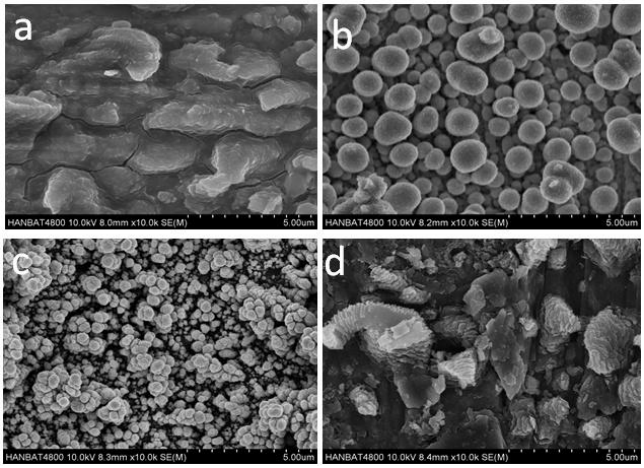

Figure 2

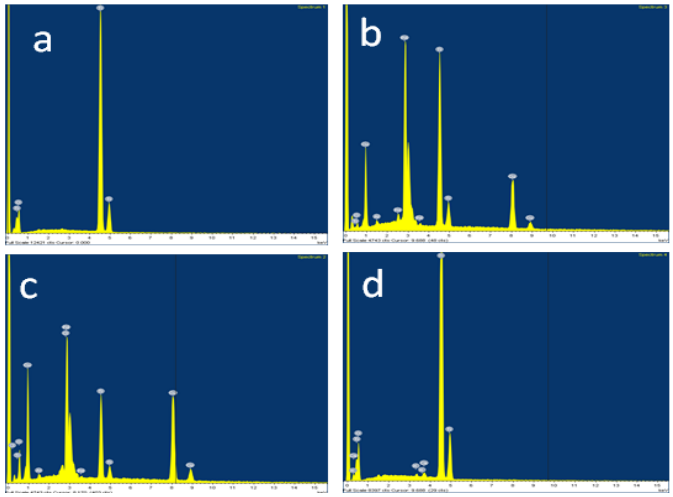

Figure 3

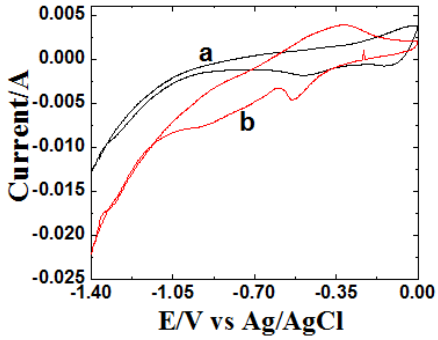

Figure 4

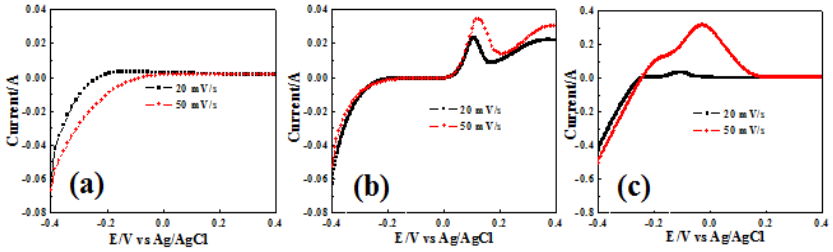

Figure 5

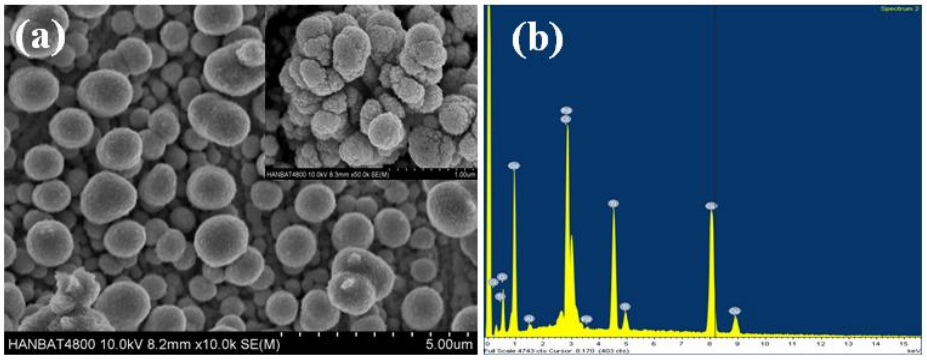

Figure 6

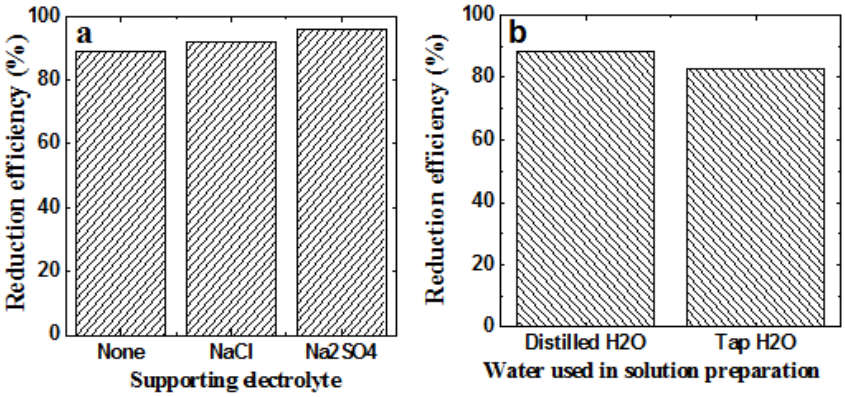

Figure 7

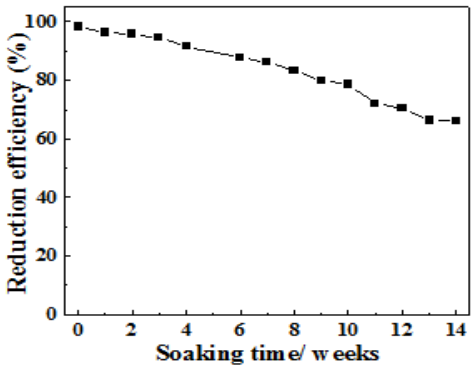

Figure 8

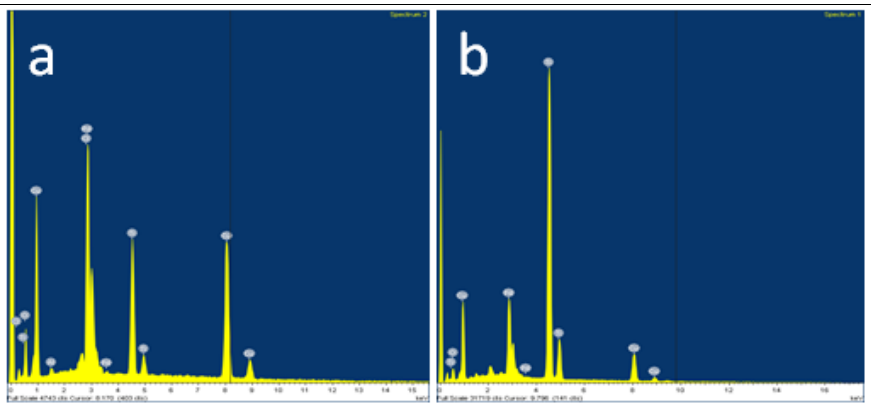
a
b